ECS 1595c

0955-2219(95)00104-2

Journal of the European Ceramic Society **16** (1996) 55–62

0955-2219/96/$15.00

Determination of the Active-to-Passive Transition in the Oxidation of Silicon Carbide in Standard and Microwave-Excited Air

Marianne J. H. Balat

Institut de Science et de Génie des Matériaux et Procédés (I.M.P. - C.N.R.S.), BP 5, 66125 Font-Romeu, Odeillo, France

(Received 27 January 1995; revised version received 31 May 1995; accepted 31 May 1995)

Abstract

The active-to-passive transition is determined on sintered silicon carbide for two atmospheres: standard air and air excited by microwaves, as a function of oxygen partial pressure and temperature. The experiments were done at low total pressure ranging from 10^3 to 25×10^3 Pa and at high temperature from 1385 to 1765°C at a constant air flow rate. The results are compared with literature data and we try to explain why they are so many differences between all the experimental and theoretical results.

1 Introduction

Silicon carbide is used as a protective material of carbon/carbon or carbon/silicon carbide composites for the nose cap and the wing leading edges of the space shuttle to prevent high temperature oxidation. During the atmospheric re-entry of hypersonic vehicles, the shock wave produces excited species (ions, atoms, molecules, electrons) and a convective thermal flux which lead to chemical and physical attacks of the protective material. So it is necessary to determine the conditions of pressure and temperature at which a non-reversible degradation of the silicon carbide occurs using an experimental device working close to realistic re-entry conditions.

The oxidation of silicon carbide is divided in two regimes separated by the transition zone: (i) the passive oxidation with the formation of a silica layer on the SiC surface, resulting in a net mass increase according to:

$$SiC(s) + 3/2O_2(g) \rightarrow SiO_2(s) + CO(g); \quad (1)$$

(ii) the active oxidation, at higher temperature with vaporization of the two oxides SiO and CO leading to a net weight loss according to:

$$SiC(s) + O_2(g) \rightarrow SiO(g) + CO(g). \quad (2)$$

First, we have made a theoretical thermodynamic calculation based on the models of Eriksson[1] and Wagner.[2] The Eriksson's model (SOLGASMIX) is based on the free-energy minimization method for a constant temperature and pressure values. The constraints of the model are: closed system, mass conservation and Duhem's phase rule. Wagner's model, modified for silicon carbide, is well suited because it takes into account the mass transfer constraints (open system) with the hypothesis of diffusion limitation type and leads to an analytical determination of the transition point in terms of oxygen partial pressure in the bulk gas for each temperature.

For each phase (solid, gaseous), the mass balance for each atomic compound is established and then the interface mass conservation (steady state). The flux density J_i of compound i at the interface is expressed by Fick's law:

$$J_i = -D_i(P_i^{\infty} - P_i^{w})/\delta_i RT, \quad (3)$$

with D_i the mass transfer coefficient of i in the carrier gas N_2, $D_i = D_{i,N_2}$, δ_i the thickness of the boundary concentration layer, R the ideal gas constant, T the temperature, P_i the partial pressure of the species i in the bulk gas (P_i^{∞}) and at the interface (P_i^{w}). So we obtain (superscript G is used for the gaseous phase):

$$J_{O_2}{}^{G} + J_{SiO}{}^{G} = 0 \text{ and } J_{N_2}{}^{G} = 0. \quad (4)$$

With the two hypotheses: $P_{O_2}{}^{w} = 0$ (interface consumption) and $P_{SiO}{}^{\infty} = 0$ (boundary layer concentration) and according to Wagner's approximation about the ratio of the thicknesses (for a laminar flow, here $Re < 1$,) we obtain:

$$P_{O_2}{}^{\infty} = (D_{SiO}/D_{O_2})^{1/2} \cdot P_{SiO}{}^{w}. \quad (5)$$

Then the oxygen partial pressure is expressed in terms of thermodynamical parameters accounting for the equilibria (1) and (2) with the two constants K_1 and K_2 defined by:

Table 1 Oxygen partial pressure and temperature for the active to passive theoretical transition in the oxidation of silicon carbide

T(K)	1473	1573	1673	1773	1873	1973	2073
$P_{O_2}^{\infty}$(Pa)	9	57	297	1242	4410	13628	37558

$$K_1 = \exp(-\Delta G_1°/RT) = P_{CO}{}^{w} \cdot (P_{O_2}{}^{w})^{-3/2} \quad (6)$$

$$K_2 = \exp(-\Delta G_2°/RT) = P_{SiO}{}^{w} \cdot P_{CO}{}^{w}/P_{O_2}{}^{w}. \quad (7)$$

Finally, the oxygen partial pressure of transition in the bulk is:

$$P_{O_2}{}^{\infty} = \left(\frac{D_{SiO}}{D_{O_2}}\right)^{3/8} \left(\frac{D_{CO}}{D_{O_2}}\right)^{1/8} K_2^{3/4} K_1^{-1/2}. \quad (8)$$

In the case of an ideal gas at low density, the diffusion coefficient can be approximated by the Chapman–Enskog theory.[3] For the equilibrium constants, the JANAF[4] tables were used. Table 1 gives the values of temperature and pressure for the transition.

In terms of $P_{O_2}{}^{\infty}$ equivalent, the same result for the transition is obtained in the case of atomic oxygen.[5]

2 Literature Data

Many authors have worked on the determination of the transition[6–19] (Table 2) but the results are very different and now we try to explain the observed differences according to:

— for theoretical calculations: the enthalpies and the diffusion coefficient values;

— for experimental results: the nature of the silicon carbide, the composition and the gas flow, the partial and total pressures, the temperature level and measurement, the method used and the criterion taken for transition (presence of bubbles, passivation by silica or only presence of a silica layer, etc.).

2.1 Theoretical comparison

Various authors[5–8] have worked on the theoretical determination of the transition line (Fig. 1). We have used the Wagner's model as has Singhal, but the differences observed between the two results result from:

— the values taken for the formation enthalpies of SiC (Janaf tables of 1971 and 1985) have a difference of nearly 30%: at 2100 K, $\Delta G_f°$(SiC) = 58·162 kJ/mol in 1971 and 44·738 in 1985;

— the value of the diffusion coefficients D_{SiO} and D_{O_2}: the ratio D_{SiO}/D_{O_2} is equal to 0·16 for Singhal and 0·44 for us, leading to a difference of 47%.

For nickel,[7] the explanation is very different because the role of condensed SiO(l) is taken into

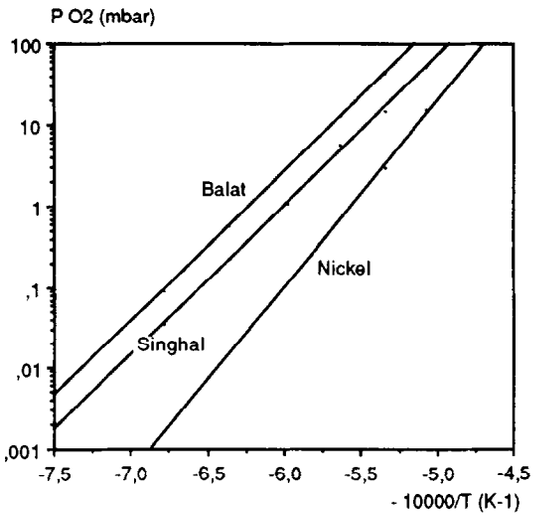

Fig. 1. Oxygen partial pressure versus temperature for the active to passive transition of SiC — theoretical determination.

Table 2. Literature data, tests conditions and materials used for the studies on the active to passive transition in the oxidation of silicon carbide

Authors	*SiC material*	*Gas*	*Flow (cm^3/s)*	*P_{O_2} (Pa)*	*P total (Pa)*	*Method*	*Range T (°C) measure*
Singhal[6]	—	O_2	—	—	—	theory	—
Nickel[7]	—	O_2	—	—	—	theory	—
Heuer[8]	—	O_2	—	—	—	theory	—
Balat[5]	α and β	$O_2 + N_2$	—	—	—	theory	—
Gulbransen[9]	monocrystal α 6H	O_2	static	1–100	1–100	TGA	927–1520 thermocouple
Hinze[10]	HP β	O_2 + Ar	1·42	5·5–932	2×10^4	TGA	1350–1550 thermocouple
Vaughn[11]	sintered α + C, B, N	Dry air (without H_2O)	0·17–1·66	2·5–125	12·5–625	TGA	1350–1550 thermocouple
Narushima[12]	CVD β	O_2 + Ar	1·42–12·50	6–500	10^5	TGA	1567–1650 thermocouple
Dickinson[13]		$O_2 + N_2$			10^5		
Keys[14]	sintered	Dry O_2	static	$1·3–9·3 \times 10^4$	$1·3–9·3 \times 10^4$	TGA	1300–1500
Pampuch[15]	CVD	O_2	2·77	10^5	10^5	furnace	
Rosner[16]	CVD β	$O_2 + N_2$	20	0·4–133	133	TGA	1477–2127
	on W filament	O	20	0·01–6·65			opt. pyrometry
Balat	sintered α 6H	air	1·11	$200–5 \times 10^3$	$10^3–2·5 \times 10^4$	solar	1385–1765
	and CVD	O_2,N_2, O, etc.	1·11	$200–10^3$	$10^3–5 \times 10^3$	furnace	opt. pyrometry

account and also the carbon activity. At high carbon activities, the incompatibility between silicon carbide and silica determines the transition while at lower carbon activities and at high temperatures, the incompatibility between SiC and SiO(l) marks the transition. Moreover, the chemical interaction in the layer SiO(l)–SiO_2 layer could cause bubbles formation at 1700–1800°C due to the CO pressure value. For Heuer,[8] the theoretical calculation using the volatility diagrams for the Si–O–C system leads to a same result as us (one value given for 1427°C).

2.2 Experimental results on sintered SiC

Various authors[9,10,11,14] have worked on the determination of the transition zone on sintered materials (Fig. 2). Gulbransen *et al.*[9] consider three possible thermodynamical equilibria for the transition reported here:

$$\text{(eqn A)}\quad SiC(s) + 2SiO_2(s) \rightarrow 3SiO(g) + CO(g) \quad (9)$$

$$\text{(eqn B)}\quad SiC(s) + SiO_2(s) \rightarrow 2SiO(g) + C(s) \quad (10)$$

$$\text{(eqn C)}\quad 2SiC(s) + SiO_2(s) \rightarrow 3Si(s) + 2CO(g). \quad (11)$$

Doing experiments, they conclude that the active/passive transition is best described by equilibrium (C) (relation 11), but in our case, we have never found solid silicon or graphite in the products, so we think that the correct transition is determined by the equilibrium (A). The experimental results we have obtained with silicon carbide are in agreement with equilibrium (A) (Fig. 2).

Moreover, the transition is introduced by the interaction of silicon carbide and silica, this is not really correct because it is preferable to study the interaction of solid silicon carbide with the gaseous phase (pure oxygen or a mixture containing oxygen). They also suggest that the transition is sensible to the total pressure, to the presence of an inert gas and to the counterflow mass balance conditions in the boundary layer.

The results of Hinze *et al.*[10] are also different. This may be due to the nature of the silicon carbide (β-SiC polycrystalline HP), and the nature of the gas (Ar + O_2) at a total pressure of 2×10^4 Pa, higher than those used by Gulbransen, Vaughn and us.

The results of Keys[14] show the same behavior as Hinze's, this may be explained by the same total high pressure range.

For Vaughn and Maahs,[11] the position of the transition is linked to the gas flow rate, moreover the conditions given before. The transition temperature, for a given partial pressure moves towards higher temperatures as the flow rate is increased. The reported values for Vaughn in Fig. 2 are given for the higher gas flow of 1·66 $cm^3\ s^{-1}$, near the one we have used.

2.3 Experimental results on CVD SiC

We, Narushima,[12] Rosner[16] have worked with CVD β-silicon carbide (Fig. 3). The results are also different essentially according to the total pressure used. Rosner worked at very low total pressure (133 Pa max) so the transition could be influenced by the pressure level (molecular gas flow regime). The pressure range of Narushima and us is closely related, so the difference between the experimental results is not so important. Narushima gives several values according to the gas flow (from 1·42 to 12·5 $cm^3\ s^{-1}$) and the results are very far from the others. This difference in the position of the transition line is attributed to a non-equilibrium state at the SiC surface when the gas flow rate increases too much.

The shift between the three curves can be explained by the total pressure level. The theoretical

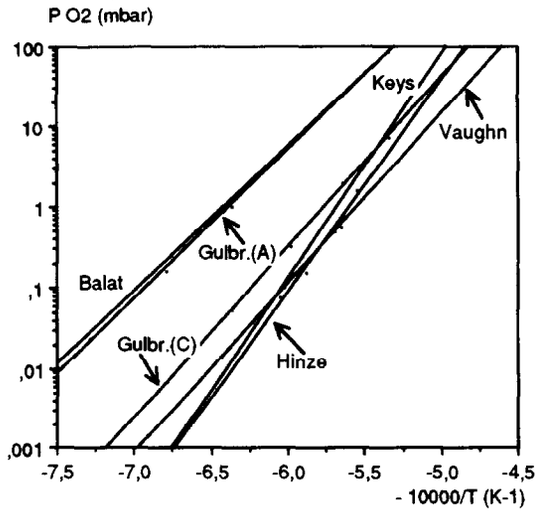

Fig. 2. Oxygen partial pressure versus temperature for the active to passive transition of SiC under standard atmosphere — experimental determination for sintered silicon carbide.

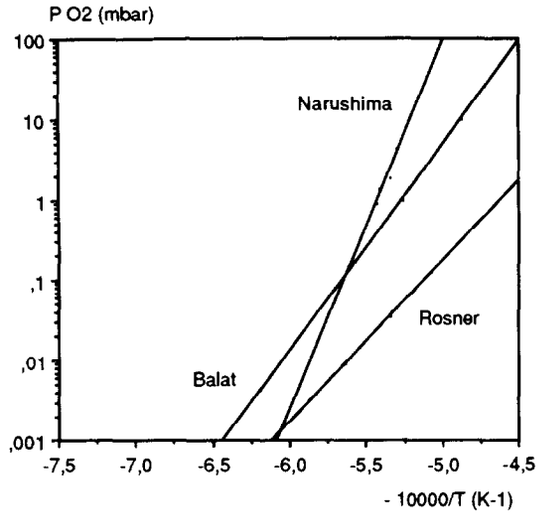

Fig. 3. Oxygen partial pressure versus temperature for the active to passive transition of SiC under standard atmosphere — experimental determination for CVD silicon carbide.

line (Wagner's model) is located at lower temperature for a fixed pressure, this model being based on the hypothesis of a diffusion limitation type. In Table 2, the total pressures are increasing from Rosner to Narushima, so probably the control of the reaction is a kinetic one for them. By increasing the total pressure, the line will be displaced towards low temperature, going to a diffusion reaction control.

2.4 Experimental results under dissociated atmosphere

Only Rosner[16] and us have worked under atomic oxygen to determine the transition (Fig. 4) in order to simulate atmospheric re-entry environment. The main differences are

— gas nature: in Rosner's case, the initial medium is made of 3% nitrogen and 97% argon, then a microwave discharge (at P = 133 Pa) is created to liberate atomic nitrogen which reacts in post-discharge with nitrogen monoxide giving atomic oxygen and molecular nitrogen;

— silicon carbide nature: sintered (so with binding material) or CVD SiC on C/SiC material in our case and CVD SiC on W filament for Rosner;

— gas flow: 1·11 $cm^3\ s^{-1}$ in our case and 20 $cm^3\ s^{-1}$ for Rosner, this acts on the oxygen dissociated concentration.

The shift between the experimental straight lines may be due to the nature of the reactive gas (pure atomic oxygen for Rosner) and also, as we have seen before, to the total pressure level.

3 Experimental Procedure

Figure 5 represents the experimental set-up called MESOX (Moyen d'Essai Solaire d'OXydation)

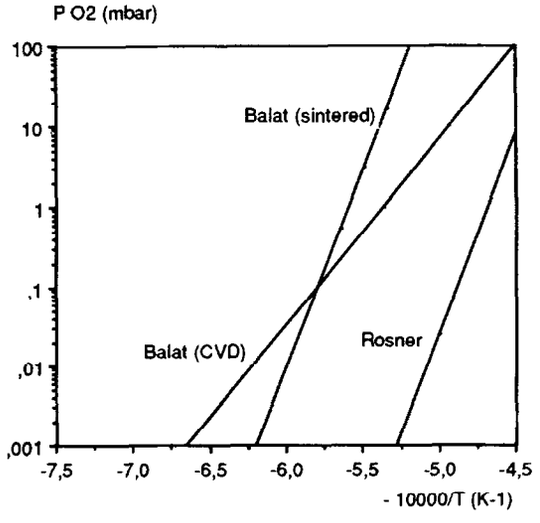

Fig. 4. Oxygen partial pressure versus temperature for the active to passive transition of SiC — experimental determination under excited air (Balat) or atomic oxygen (Rosner).

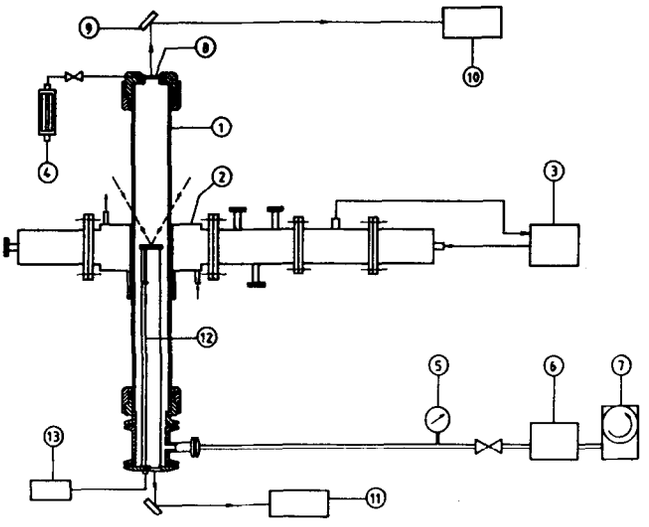

Fig. 5. Experimental set-up: (1) silica vessel, (2) wave guide, (3) microwave generator, (4) flowmeter, (5) manometer, (6) pressure regulator, (7) vacuum pump, (8) viewport, (9) mirror, (10) optical pyrometer, (11) spectroradiometer, (12) optical fiber probe, (13) bi-chromatic pyrometer.

which associates a solar radiation concentrator (to heat up samples to 2300°C for diameters of 25 mm min and 40 mm max) to a microwave generator (for the gas dissociation). The total pressures are between 10^2 and 10^5 Pa. This set-up was chosen to test samples in conditions closed to those encountered during an atmospheric reentry of space shuttles (very different from TGA measurement).

The device is composed of a silica cylindrical vessel (Φint = 50 mm, 500 mm high) which crosses the refrigerated wave guide. Inside the vessel, a zirconia tube with a zirconia sample-holder supports the materials. The microwave generator (0–1200 W, 2450 MHz) works at a constant power of 300 W for the results presented. The incident and reflected powers are measured. The device is placed at the focus of a solar furnace, the heat fluxes can reach 3·5 MW/m^2, thus elevated temperatures on materials such as SiC may be obtained. A regulator and a gauge are used in order to control precisely the pressure during the experiment. An optical pyrometer equipped with a filter centred at 5.5 μm gives the color temperature. The measure is performed with a CaF_2 viewport and a mirror. The correction of the temperature due to the emittance is done *a posteriori* with a value of 0·90 for SiC and SiO_2 at this wavelength.[20] The uncertainty in the temperature due to the emittance correction is ± 1·5% at 1500°C for a variation of ± 5% on ϵ. An original optical fiber probe with a sapphire rod is linked to a bi-chromatic pyrometer for the temperature measurement of the rear face (= without sun) of the sample.

The atomic oxygen concentration (in the ground state $2P^3P_J$ with J = 2, 1, 0) was estimated

by Laser Induced Fluorescence (LIF) at 5 cm from the microwave discharge with an accuracy of ± 20%. For an input power of 300 W and for a gas flow of 1.11 $cm^3 s^{-1}$, the atomic oxygen concentration is comprised between 5×10^{11} and $8{\cdot}5 \times 10^{13}$ at· cm^{-3} when the total pressure goes from 600 to 5000 Pa.

4 Results and Discussion

The cylindrical samples are sintered α-SiC (6H) (density $3{\cdot}15 \times 10^3$ kg/m^3, theoretical value: $3{\cdot}21 \times 10^3$ kg/m^3) containing as major impurities 1% B, less than 2000 ppm Si and SiO_2, and less than 1000 ppm of Fe, C and (Na+K+Ca+Mg). The sample dimensions are 25 mm diameter and 3 mm high. The upper face (exposed to the solar radiation) is polished using a 1 μm diamond polishing compound, then cleaned ultrasonically in acetone and ethanol and dried before testing.

The CVD SiC samples are composite structures provided by a French society, S.E.P. (Société Européenne de Propulsion). They are 2D C/SiC composites with a coating of CVD β SiC and they tested as received. The sample dimensions are the same.

4.1 Experimental protocol

Before each experiment, the pressure and the air flow ($1{\cdot}11$ $cm^3 s^{-1}$) are fixed. For the experiments performed under plasma, the plasma is started after the pressure stabilization and before solar heating. The gradual opening of a shutter placed between the sample and the concentrated solar radiation allows the control of the temperature level. The thermal history of each sample is represented in Fig. 6 with a temperature increase of 4°/s then a plateau of nearly 400 s and finally a decrease at a rate of 2°/s. The duration of the plateau is large enough to indicate the active oxidation regime. In fact, during the temperature raising and decreasing at every pressure, silica formation takes place. But on the temperature plateau, when active oxidation occurs, the surface of silicon carbide is very damaged and the silica formation when decreasing the temperature does not affect the phenomenon as SEM micrographs reveal.

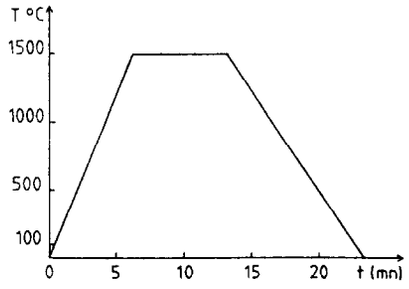

Fig. 6. Thermal history of the sample.

The modification of the sample is controlled by weighing, X-ray diffraction (XRD), scanning electron microscopy (SEM) and Ayers spectroscopy.

4.2 Experiments under standard air for sintered SiC

The results are presented in Fig. 7. For samples (●), after the oxidation test run, the surface is covered with a very thin passive silica layer, the mass gain being weak. For other samples (○), the surface after oxidation is damaged with a very large specific area (Fig. 8(c)). The relative mass losses are comprised between 0·1 and 3·6%. These results under standard air are in good agreement with the thermodynamic calculation (straight line Th.).

4.3 Experiments under microwave-excited air for sintered SiC

The results are presented in Fig. 7 and are far from those predicted by thermodynamics. All (▲) samples have a passive silica layer after oxidation. For a sample located far from the transition line, the thickness of the silica layer is about 150 nm. For other samples after oxidation, the surface is very damaged and as previously the surface is very divided (Fig. 8 (e)). The relative mass losses are comprised between 1 and 4%. In the case of dissociated air, the transition zone is located at lower pressure for the same temperature. So, the dissociation significantly enlarges the p–t domain characterized by the presence of a passive silica layer. The great difference observed between the results and theory may be attributed to out-of-equilibrium phenomena and/or kinetics surface activation.

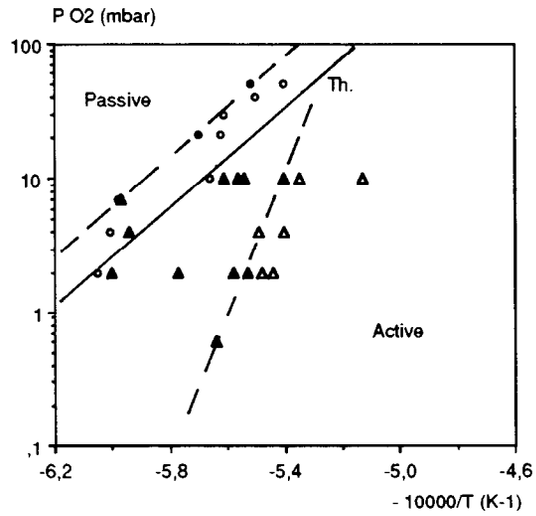

Fig. 7. Oxygen partial pressure versus temperature for the active to passive transition of SiC under molecular (o) and dissociated (Δ) air — experimental determination for sintered silicon carbide in dotted line. ● or ▲: samples with a passive silica layer; ○ or Δ: active oxidation. The theoretical continuous line is that of Balat.

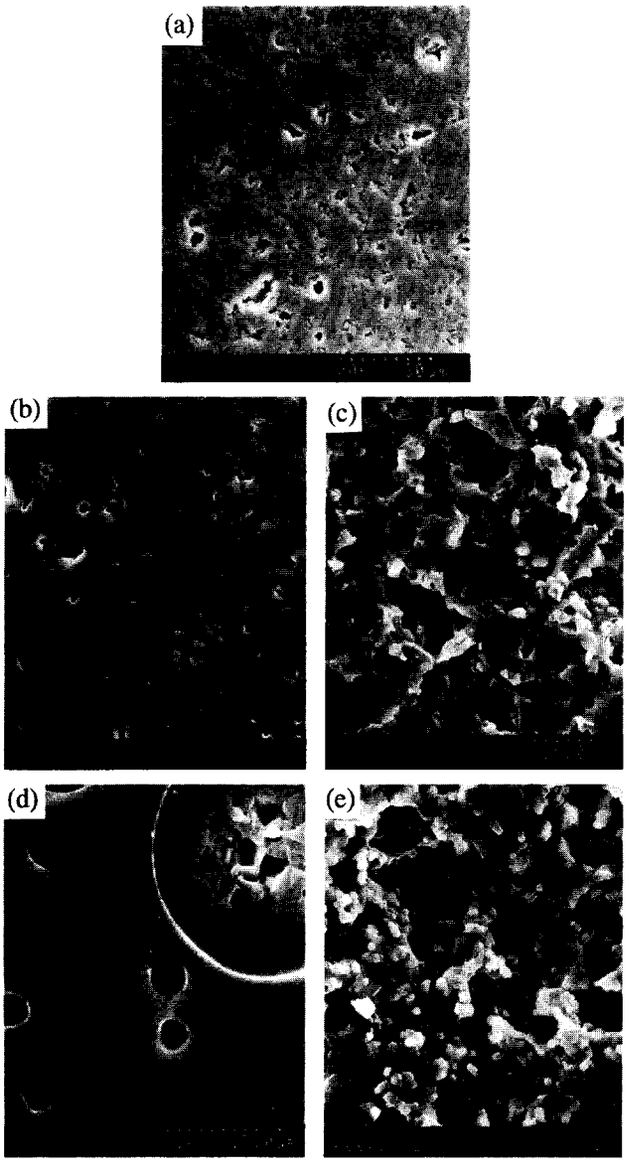

Fig. 8. SEM micrographs of sintered silicon carbide: (a) before oxidation, (b) after passive oxidation under standard air (T = 1480°C, P_{O_2} = 2·1 × 10^3 Pa), (c) after active oxidation under standard air (T = 1510°C, P_{O_2} = 3 × 10^3 Pa), (d) after passive oxidation under excited air (T = 1580°C, P_{O_2} = 10^3 Pa) and (e) after active oxidation under excited air (T = 1595°C, P_{O_2} = 10^3 Pa).

4.4 Experiments under standard air for CVD SiC on C/SiC composites

As previously, for samples (●), after the oxidation test run, the surface is covered with a very thin passive silica layer but there is always a weak mass loss for each sample (max 0·5‰ relative), this probably due to the porosity and the access of oxygen to the carbon fiber (Fig. 9). Thus the mass loss is not always representative of an active oxidation, it depends on the nature of the material (substrate + coating). The surface observation by SEM provides better information on the active to passive transition. For other samples (○), the surface after oxidation is very damaged, so the oxidation regime is active. The relative mass losses are comprised between 0·7% and 2·9%.

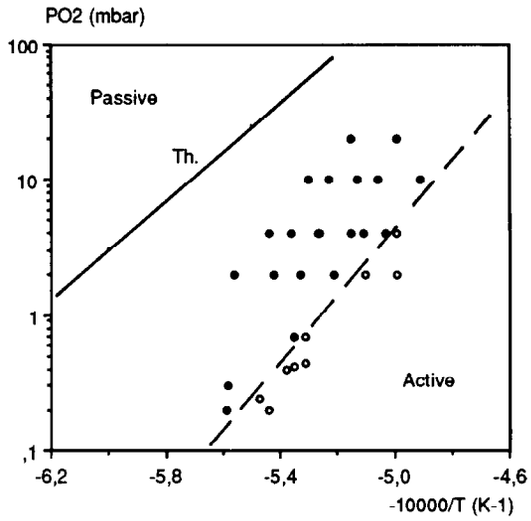

Fig. 9. Oxygen partial pressure versus temperature for the active to passive transition of SiC under standard air (○) — experimental determination for CVD silicon carbide in dotted line. ●: samples with a passive silica layer; o: active oxidation. The theoretical continuous line is that of Balat.

The results are very far from the thermodynamic calculation and this behavior is very different from the one obtained with the sintered silicon carbide.

Figure 10 presents SEM micrographs of samples before treatment (sample 3200), in the passive region (sample 3406) and in the active one (sample 3206). The silicon carbide is very damaged on the sample 3206 and the bare carbon fibers can be seen.

4.5 Experiments under microwave-excited air for CVD SiC on C/SiC composites

The results are presented in Figure 11. All (▲) samples have a passive silica layer after oxidation with very weak mass losses. For other samples (Δ), after oxidation, the surface is damaged (active regime). The relative mass losses are comprised between 0·8% and 3·1%.

The observed difference between the standard and excited atmospheres is very weak (about 20–30° in the studied pressure range). It seems that, contrary to sintered silicon carbide and the results of Rosner, the use of atomic oxygen decreases the passive zone. So this behavior shows the importance of the nature of the silicon carbide on the position of the transition line.

Figure 10 shows SEM micrographs of samples in the passive zone (sample 3390) and in the active one (sample 3203). The active oxidation takes place in the cracks of the silicon carbide layer.

5 Conclusions

The active to passive transition in the oxidation of silicon carbide is examined for two kinds of mate-

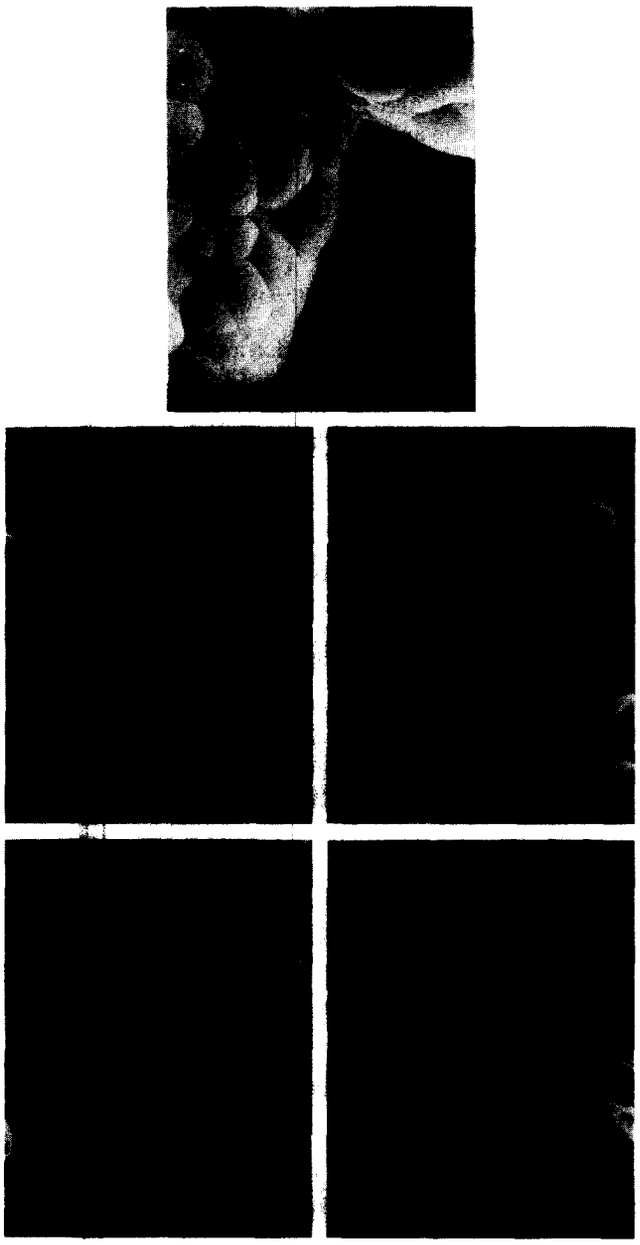

Fig. 10. SEM micrographs of CVD β silicon carbide (3200) before oxidation, (3406) after passive oxidation under standard air (T = 1646°C, P_{O_2} = 200 Pa), (3206) after active oxidation under standard air (T = 1687°C, P_{O_2} = 200 Pa), (3390) after passive oxidation under excited air (T = 1740°C, P_{O_2} = 10^3 Pa) and (3203) after active oxidation under excited air (T = 1758°C, P_{O_2} = 10^3 Pa).

rials (sintered and CVD) under standard and atmospheric re-entry conditions and compared to the literature data. Several differences in the results are observed due to the nature of the silicon carbide, the gas flow rate and its nature, and the total pressure used.

The influence of the total pressure level is very important and can explain the control of the reaction (kinetic or diffusion limitation) and so the position of the transition line. It is necessary to do more experiments at higher total pressure to find out its role, the transition line will be moved towards the theoretical calculation (under diffusion control).

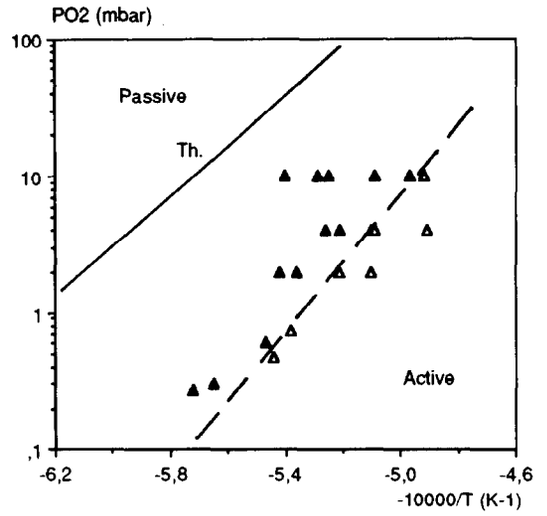

Fig. 11. Oxygen partiail pressure versus temperature for the active to passive transition of SiC under excited air Δ — experimental determination for CVD silicon carbide in dotted line. ▲: samples with a passive silica layer; Δ: active oxidation.

Moreover, to show the influence of the silicon carbide nature, several experiments will be done on CVD SiC (made in our laboratory) deposited on sintered SiC. It is also necessary to understand the differences observed between the two atmospheres (standard and excited) on the position of the transition zone.

Acknowledgement

The author wants to thank the S.E.P. society for the authorization of publication of industrial results and for its financial support of this work (Contract 487210).

References

1. Eriksson, G., Thermodynamic studies of high temperature equilibria XII Solgasmix. *Chem. Scrip.*, **8** (1973) 100–3.
2. Wagner, C., Passivity during the oxidation of silicon at elevated temperature. *J. Appl. Phys.*, **29** (1958) 1295–7.
3. Bird, R. B., Stewart, W. E. & Lightfood, E. N., In *Transport Phenomena*. J. Wiley, New York (1960) pp. 508–13.
4. Chase, M. W., Davies J. R. *et al.*, *JANAF Thermodynamical Tables*, 3rd Ed., *J. Phys. Chem. Ref. Data*, **14** suppl. 1 (1985).
5. Balat, M., Flamant, G., Malé, G. & Pichelin G., Active to passive transition in the oxidation of silicon carbide at high temperature and low pressure in molecular and atomic oxygen. *J. Mater. Sci.*, **27** (1992) 697–703.
6. Singhal, S. C., Thermodynamic analysis of the high-temperature stability of silicon nitride and silicon carbide. *Ceramurgia*, **2** (1976) 123–30.
7. Nickel, K. G., The role of condensed silicon monoxide in the active-to-passive oxidation transition of silicon carbide. *J. Europ. Ceram. Soc.*, **9** (1992) 3–8.
8. Heuer, A. H. & Lou, V. L., Volatility diagrams for silica, silicon nitride and silicon carbide and their application to high-temperature decomposition and oxidation. *J. Am. Ceram. Soc.*, **73** (1990) 2789–803.
9. Gulbransen, E. A. & Jansson, S. A., The high-temperature

oxidation, reduction and volatilization reactions of silicon and silicon carbide. *Oxid. Met.*, **4** (1972) 181–201.
10. Hinze, J. W. & Graham, H. C., The active oxidation of silicon and silicon carbide in the viscous gas-flow regime. *J. Electrochem. Soc.*, **123** (1976) 1066–73.
11. Vaughn, W. L. & Maahs, H. G., Active-to-passive transition in the oxidation of silicon carbide and silicon nitride in air. *J. Am. Ceram. Soc.*, **73** (1990) 1540–3.
12. Narushima, T., Goto, T., Iguchi, Y. & Hirai, T., High-temperature active oxidation of chemically vapor-deposited silicon carbide in $Ar–O_2$ atmosphere. *J. Am. Ceram Soc.*, **74** (1991) 2583–6.
13. Dickinson, R. C., Oxidation protection. In *Proceedings of the Oxidation-Resistant Carbon–Carbon Composites for Hypersonic Vehicle Application Workshop*, Hampton VA, Sept. 1987, NASA Conf. Public. 2501, pp. 129–41.
14. Keys, L. H., The oxidation of silicon carbide. In *Proceedings of the Symposium on Properties of High Temperature Alloys*, **77-1**, Electrochem. Soc., Princeton NJ, (1977) 681–96.
15. Pampuch, R. & Jonas, S., New aspects of the oxidation of silicon carbide. *Sci. Ceram.*, **9** (1977) 300–7.
16. Rosner, D. E. & Allendorf, H. D., High temperature kinetics of the oxidation and nitridation of pyrolytic silicon carbide in dissociated gases. *J. Phys. Chem.*, **74** (1970) 1829–39.
17. Antill, J. E. & Warburton, J. B., Active to passive transition in the oxidation of silicon carbide, *Corros. Sci.*, **11** (1971) 337–42.
18. Kim, H. E. & Moorehead, A. J., Effect of active oxidation on the flexural strength of α-SiC, *J. Am. Ceram. Soc.*, **73** (1990) 1868–72.
19. Schiroky, G. H., Oxidation behavior of chemically vapor-deposited silicon carbide, *Adv. Ceram. Mater.*, **2** (1987) 137–41.
20. Touloukian, Y. S. & De Witt, D. P., *Thermal Radiative Properties — Non Metallic Solids*, Vol. 8. Plenum Press, New-York (1972).